Proceedings of the 2003 IEEE International Frequency Control Symposium and PDA Exhibition
Jointly with the 17th European Frequency and Time Forum

DATA-INTENSIVE ANALYSIS AND CONTROL OF FLEXIBLE POINTING SYSTEMS WITH PZT ACTUATORS

Sergey Edward Lyshevski
Department of Electrical Engineering, Rochester Institute of Technology, Rochester, New York 14623-5603, USA
E-mail: seleee@rit.edu; Web: www.rit.edu/~seleee

Abstract – **We research cornerstone aspects in the design, modeling, analysis, and optimization of pointing systems. Specifically, the major objectives are encompassed on development of high-performance high-precision pointing systems with surface-mounted piezoelectric (PZT) actuators and MEMS. Pointing systems are flexible, and it is inherently difficult to stabilize and control the flexible modes and guarantee accurate pointing. Therefore, advanced actuation and sensing hardware and design paradigms must be developed and implemented. This paper focuses on the application of the PZT actuators, MEMS and high torque density brushless servomotors to attain the desired objectives. These novel actuators and sensors integrated with high-performance electronics. Performance assessment is performed through high-fidelity modeling, heterogeneous simulations, data-intensive analysis, experiments and characterizations. Robust control algorithms are designed and implemented with the ultimate objective to improve the performance, e.g., efficiency, accuracy, stability, settling time, fast retargeting, etc. Far-reaching multidisciplinary research and multi-objective optimization of interactions between beam – mechanical structures – actuators – sensors – electronics/ICs are performed. It is illustrated that advanced actuators, sensors, ICs and DSPs must be used to achieve the objectives. In particular, PZT actuators and brushless servomotors guarantee high-accuracy fast positioning, rapid retargeting and vibration attenuation. Devising of pointing system (mechanical and electronic design includes actuation and sensing hardware developments, discovery and implementation of novel actuators and sensors, optimization their location and number, integration of actuators-sensors-ICs-DSPs), analysis, modeling, design and optimization are fundamental problems. These problems are addressed and solved. This paper documents the innovative results in modeling, analysis, and control of high-performance pointing systems.**

Keywords **– control, flexible pointing system, modeling, optimization, PZT actuators, MEMS**

1. INTRODUCTION

Current and future pointing platforms [1, 2] require highly accurate pointing, fast tracking and rapid retargeting capabilities in the presence of unpredictable motions, beam flexibility and nonlinear time-varying adverse phenomena (vibration, backlash, friction, saturation, shocks, etc.). It is necessary to develop advanced DSP-ICs-actuators-beam-sensors hardware that guarantee precise and fast (minimum-time) tracking and retargeting in the presence of flexible modes, adverse effects and nonlinearities [3-6]. Other problems to be solved are hardware – software codesign, high-fidelity modeling, heterogeneous simulation, robust control, nonlinear multiobjective optimization, etc.

The coherent synergetic developments are performed in this paper, and the results reported are directed towards thorough analysis and design of high-performance turreted pointing systems. The key advantage of the concept reported is the fact that one directly and non-conservatively incorporates the qualitative and quantitative knowledge of hardware and software as well as integrates the adverse phenomena (vibration, nonlinearities, constraints, friction, hysteresis, etc.) in the analysis and design. The accurate knowledge of disturbances, vibrations, misalignments, complex nonlinear phenomena, parameter variations and other quantities are frequently not known precisely. Furthermore, mathematical models are simplified to make analysis, design, simulation and optimization computationally tractable. Correspondingly robust controllers must be designed to cope with system nonlinearities, time-varying uncertainties, etc. The design concept reported significantly departs from other methods [7-9]. It is illustrated that it is possible to guarantee precise tracking, fast retargeting, attenuate (minimize) vibrations and disturbances, as well as reduce the degrading effects of nonlinearities, constraints, parameter variations and uncertainties. The proposed concept provides the coherent method in robust design to achieve accurate fast positioning, rapid retargeting, stability, robustness, and disturbance attenuation.

A novel hardware design that utilizes advanced actuation – sensing paradigms (surface-mounted PZT actuators, MEMS actuators and sensors, direct-drive servomotors) with matching electronics/ICs is proposed and verified. We depart from conventional actuation and sensing technologies. The devised solution allows one to achieve fast and accurate positioning, actively attenuate vibrations and disturbances. In addition to the experimental research, applied and fundamental research is performed. In particular, high-fidelity mathematical models developed guarantee data-intensive analysis with coherent assessment analysis with outcome prediction. This paper synthesizes and studies nonlinear roust control laws for high-performance pointing systems through algorithms and theory developments, real-time hardware-in-the-loop tests, as well as software and hardware developments. The closed-loop system performance is examined through nonlinear simulations and experiments. Our efforts lead one to the development of advanced computationally efficient software and state-of-the-art hardware. The research contributes to control, advanced actuation and sensing hardware, and novel computer-aided-design tools design to reuse, prototype and advance developments of different pointing systems. The contributions are documented through explicit demonstrations and results verifications.

II. POINTING SYSTEM HARDWARE

The pointing system with a flexible beam controlled by surface-mounted PZT actuators and brushless permanent-magnet synchronous servomotor in the horizontal and vertical axes is documented in Figure 1.

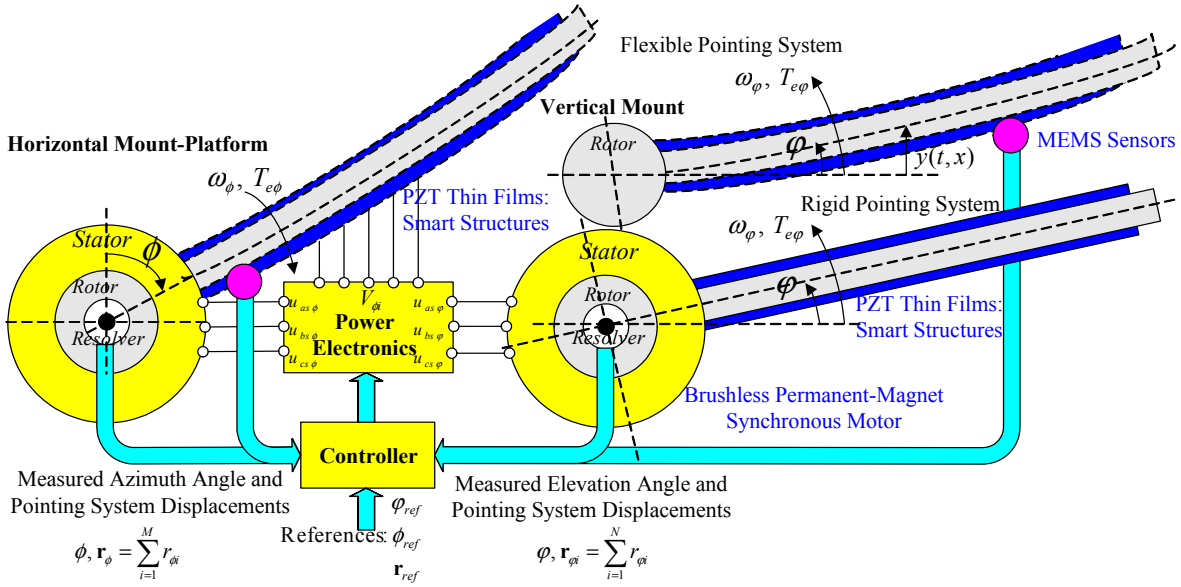

Figure 1. Pointing system in the horizontal and vertical axes

The angular displacement and position are measured using MEMS-based sensors. In the horizontal and vertical axes, the pointing system with two mounts is actuated by two brushless direct-drive permanent-magnet synchronous servomotors as illustrated in Figures 1 and 2.

Figure 2. Two-axis pointing system with direct-drive servomotors

However, the direct-drive servomotors cannot guarantee the desired positioning accuracy, attenuate vibrations, compensate nonlinearities, etc. Therefore, PZT actuators are used to attain the above mentioned objectives. These surface-mounted PZT actuators (composite PZT structures controlled using ICs) will attenuate vibrations, disturbances and flexible modes with the ultimate objective to attain stabilization and tracking of the flexible beam. Micro-positioning and accurate pointing are achieved by displacing PZT actuators. The surface-mounted PZT thin-film strips are fabricated applying the sputtering fabrication processes [10, 11]. Depending upon the composite films thickness, fabrications processes and chemicals, different performance was observed and reported in [10].

The tracking control problem must be solved to achieve micro-positioning and accurate pointing. The error vector

$$e_{\mathbf{r}}(t) = \mathbf{r}_{ref}(t) - \mathbf{r}(t)$$

is used. Here, the reference commands to *N* and *M* actuators in the horizontal and vertical axes

$$\mathbf{r}_{ref} = \begin{bmatrix} \mathbf{r}_{ref\varphi} \\ \mathbf{r}_{ref\phi} \end{bmatrix} = \begin{bmatrix} \sum_{i=1}^{N} r_{iref\varphi} \\ \sum_{i=1}^{M} r_{iref\phi} \end{bmatrix} \text{ and } \mathbf{r} = \begin{bmatrix} \mathbf{r}_{\varphi} \\ \mathbf{r}_{\phi} \end{bmatrix} = \begin{bmatrix} \sum_{i=1}^{N} r_{i\varphi} \\ \sum_{i=1}^{M} r_{i\phi} \end{bmatrix}.$$

The blushless permanent-magnet synchronous servomotors are used to displace the horizontal mount-platform (with ± 360 degrees rotational capabilities in azimuth) and vertical mount (with –30 to +90 degrees displacement in elevation). The reference (command) angular displacements in the vertical and horizontal axes are denoted as φ_{ref} and ϕ_{ref}. The displacements φ and ϕ of two mounts are measured by high-accuracy resolvers. For direct-drive servomotor angular displacements in two axes are equal to φ and ϕ, e.g., $\theta_{r\varphi} = \varphi$ and $\theta_{r\phi} = \phi$. Using the tracking errors $e_\varphi(t) = \varphi_{ref}(t) - \varphi(t)$ and $e_\phi(t) = \phi_{ref}(t) - \phi(t)$ the controller develops PWM signals to drive high-frequency transistors of power converters regulating the magnitude of phase voltages [10, 12]. The phase voltages u_{as}, u_{bs} and u_{cs} are applied to the servomotor windings to rotate vertical and horizontal mounts. High-torque Kollmorgen D- and N-series servomotors are studied. The use of high torque density direct-drive brushless servomotors allows one to significantly increase accuracy, maximize efficiency, simplify kinematics, improve integrity, enhance packaging, eliminate gears, and attenuate undesired effects.

The PZT actuators are controlled using the measured position of the flexible beam. The MEMS-based optical and capacitive sensors are used. High-accuracy position measuring is guaranteed. The PZT actuators are controlled using the high switching frequency ICs. A complete hardware solution with DSP-based controller ensures the desired degree of overall performance for flexible pointing systems. In particular, the supervisory (high-level) and subsystems controllers are designed.

III. Direct-Drive Brushless Synchronous Servomotors

The pointing system with two mounts is actuated by brushless permanent-magnet synchronous servomotors, see Figures 1 and 2. The angular velocity and displacement vary changing the phase voltages u_{as}, u_{bs} and u_{cs}. The servomotors are modeled in the *quadrature-direct* reference frame [10].The state variables are the *quadrature-*, *direct-* and *zero*-axis currents $i_{qs}^r, i_{ds}^r, i_{0s}^r$, the angular velocity ω_r ($\omega_{r\varphi}$ and $\omega_{r\phi}$), and the angular displacement θ_r ($\theta_{r\varphi}=\varphi$ and $\theta_{r\phi}=\phi$). The control variables are the *quadrature-*, *direct-*, and *zero*-axis voltages u_{qs}^r, u_{ds}^r and u_{0s}^r.

The following nonlinear differential equations describe the stand-alone servomotor dynamics [10, 12]

$$\frac{di_{qs}^r}{dt}=-\frac{r_s}{L_{ls}+\frac{3}{2}\overline{L}_m}i_{qs}^r-\frac{r_s}{L_{ls}+\frac{3}{2}\overline{L}_m}\omega_r-i_{ds}^r\omega_r+\frac{1}{L_{ls}+\frac{3}{2}\overline{L}_m}u_{qs}^r,$$

$$\frac{di_{ds}^r}{dt}=-\frac{r_s}{L_{ls}+\frac{3}{2}\overline{L}_m}i_{ds}^r+i_{qs}^r\omega_r+\frac{1}{L_{ls}+\frac{3}{2}\overline{L}_m}u_{ds}^r,$$

$$\frac{di_{0s}^r}{dt}=-\frac{r_s}{L_{ls}}i_{0s}^r+\frac{1}{L_{ls}}u_{0s}^r,$$

$$\frac{d\omega_r}{dt}=\frac{3P^2\psi_m}{8J}i_{qs}^r-\frac{B_m}{J}\omega_r-\frac{P}{2J}T_L,$$

$$\frac{d\theta_r}{dt}=\omega_r,$$

where r_s is the phase winding resistance; L_{ls} and $\overline{L}_m$ are the leakage and magnetizing inductances; ψ_m is the amplitude of the flux linkages established by the permanent magnets; P is the number of poles; B_m is the friction coefficient; J is the moment of inertia.

To displace two mounts, one regulates the electromagnetic torques changing the phase voltages. If the voltage-fed power converters are used, the magnitude u_M of phase voltages is controlled varying the duty ratio. A balanced $qd0$ voltage set is $u_{qs}^r=\sqrt{2}u_M$, $u_{ds}^r=0$, $u_{0s}^r=0$.

The following set of differential equations is found for the vertical and horizontal axes servomotors for two mounts

$$\frac{di_{qs\varphi}^r}{dt}=-\frac{r_s}{L_{ls}+\frac{3}{2}\overline{L}_m}i_{qs\varphi}^r-\frac{r_s}{L_{ls}+\frac{3}{2}\overline{L}_m}\omega_{r\varphi}-i_{ds\varphi}^r\omega_{r\varphi}+\frac{1}{L_{ls}+\frac{3}{2}\overline{L}_m}u_{qs\varphi}^r$$

$$\frac{di_{ds\varphi}^r}{dt}=-\frac{r_s}{L_{ls}+\frac{3}{2}\overline{L}_m}i_{ds\varphi}^r+i_{qs\varphi}^r\omega_{r\varphi}+\frac{1}{L_{ls}+\frac{3}{2}\overline{L}_m}u_{ds\varphi}^r,$$

$$\frac{d\omega_{r\varphi}}{dt}=\frac{3P^2\psi_m}{8J_\varphi}i_{qs\varphi}^r-\frac{B_m}{J_\varphi}\omega_{r\varphi}-\frac{P}{2J_\varphi}T_{L\varphi},$$

$$\frac{d\theta_{r\varphi}}{dt}=\omega_{r\varphi}\ \text{ or }\ \frac{d\varphi}{dt}=\omega_{r\varphi},$$

$$\frac{di_{qs\phi}^r}{dt}=-\frac{r_s}{L_{ls}+\frac{3}{2}\overline{L}_m}i_{qs\phi}^r-\frac{r_s}{L_{ls}+\frac{3}{2}\overline{L}_m}\omega_{r\phi}-i_{ds\varphi}^r\omega_{r\phi}+\frac{1}{L_{ls}+\frac{3}{2}\overline{L}_m}u_{qs\phi}^r$$

$$\frac{di_{ds\phi}^r}{dt}=-\frac{r_s}{L_{ls}+\frac{3}{2}\overline{L}_m}i_{ds\phi}^r+i_{qs\varphi}^r\omega_{r\phi}+\frac{1}{L_{ls}+\frac{3}{2}\overline{L}_m}u_{ds\phi}^r,$$

$$\frac{d\omega_{r\phi}}{dt}=\frac{3P^2\psi_m}{8J_\phi(\phi)}i_{qs\phi}^r-\frac{B_m}{J_\phi(\phi)}\omega_{r\phi}-\frac{P}{2J_\phi(\phi)}T_{L\phi},$$

$$\frac{d\theta_{r\phi}}{dt}=\omega_{r\phi}\ \text{ or }\ \frac{d\phi}{dt}=\omega_{r\phi},$$

where J_φ and J_ϕ are the moments of inertia, and J_ϕ is the nonlinear function of the elevation angle; $T_{L\varphi}$ and $T_{L\phi}$ are the disturbances (load) torques

IV. Beam Mathematical Model

Examining the flexible beam, the following partial differential equation are used to models the beam displacement (deflection) as a function of applied point forces developed by N surface-mounted PZT actuators [3-5]

$$\frac{\partial^2 w}{\partial t^2}+2\zeta\sqrt{\frac{EI}{\rho A}}\frac{\partial^3 w}{\partial x^2\partial t}+\frac{EI}{\rho A}\frac{\partial^4 w}{\partial x^4}$$
$$=\frac{1}{\rho A}\sum_{j=1}^{N}\delta(x-x_{bj})f_{j,x_{bj}}(t)+\frac{1}{\rho A}f_d(t,x),$$

where $w(t,x)$ is the beam deflection; x is the beam coordinate; x_{bj} are the positions of the applied point forces $f_{j,x_{bj}}(t)$; $\delta(x)$ is the Dirac delta-function; $f_d(t,x)$ is the disturbance force.

The expression for the beam deflection is

$$w(t,x)=\sum_{i=1}^{\infty}\Phi_i(x)\eta_i(t),$$

where $\Phi_i(x)$ are the eigenfunctions; $\eta_i(t)$ are the dimensionless modal coordinates.

Using the modal coordinates $\eta_i(t)$, one obtains [4-6]

$$\ddot{\eta}_i+2\zeta\omega_i\dot{\eta}_i+\omega_i^2\eta_i=\sum_{j=1}^{N}\Phi_i(x_{bj})f_{j,x_{bj}}(t),$$

where $\omega_i=\left(\frac{i\pi}{l}\right)^2\sqrt{\frac{EI}{\rho A}}$ and $\Phi_i(x_{bj})=\sqrt{\frac{2}{l}}\sin\frac{i\pi x_{bj}}{l}$.

For large n, we have $w_j=\sum_{i=1}^{n}\Phi_i(x_{bj})\eta_i$.

Using the state-space model, and denoting $x_{i1}=\eta_i$, the system of differential equations is

$$\dot{x}_{i1}=x_{i2},$$

$$\dot{x}_{i2}=-\omega_i^2x_{i1}-2\zeta\omega_ix_{i2}+\sum_{j=1}^{N}\Phi_i(x_{bj})f_{j,x_{bj}}(t).$$

In the matrix form, one finds

$$\begin{bmatrix}\dot{x}_1\\ \vdots\\ \dot{x}_n\end{bmatrix}=$$

$$\begin{bmatrix}\omega_1 & 0 & 0\\ 0 & \ddots & 0\\ 0 & 0 & \omega_n\end{bmatrix}\begin{bmatrix}x_1\\ \vdots\\ x_n\end{bmatrix}+\begin{bmatrix}0 & 0 & \cdots & 0 & 0\\ \Phi_1(x_{b1}) & \Phi_1(x_{b2}) & \cdots & \Phi_1(x_{bN-1}) & \Phi_1(x_{bN})\\ \vdots & \vdots & \ddots & \vdots & \vdots\\ 0 & 0 & \cdots & 0 & 0\\ \Phi_n(x_{b1}) & \Phi_n(x_{b2}) & \cdots & \Phi_n(x_{bN-1}) & \Phi_n(x_{bN})\end{bmatrix}\begin{bmatrix}f_1\\ \vdots\\ f_N\end{bmatrix},$$

$$\begin{bmatrix}w_1\\ \vdots\\ w_N\end{bmatrix}=\begin{bmatrix}\Phi_1(x_{b1}) & 0 & \cdots & \Phi_n(x_{b1}) & 0\\ \vdots & \vdots & \ddots & \vdots & \vdots\\ \Phi_1(x_{bN}) & 0 & \cdots & \Phi_n(x_{bN}) & 0\end{bmatrix}\begin{bmatrix}x_1\\ \vdots\\ x_n\end{bmatrix},$$

where $x_i=\begin{bmatrix}x_{i1}\\ x_{i2}\end{bmatrix}$; $\omega_i=\begin{bmatrix}0 & 1\\ -\omega_i^2 & -2\zeta\omega_i\end{bmatrix}$; $\Phi_i(x_{bj})$ is the ith mode of vibration.

V. Mathematical Model of Pointing Systems With PZT Actuators

In order to position the beam as well as to attenuate vibrations and disturbances, the surface-mounted PZT actuators are placed along the beam. These actuators develop forces acting at the specific positions (we assume that ideal point forces are applied). Actuator nonlinearities and hysteresis effect are the major factors that influence the system performance. The resulting force is found as [4,5,13]

$$f_{j,x_{bj}}(t)=f_{aj,x_{bj}}+f_{ahj,x_{bj}}=k_a d_a V_j-k_a z_j,$$

where $f_{aj,x_{bj}}$ is the force developed by jth actuator, $f_{aj,x_{bj}}=k_a d_a V_j$; $f_{ahj,x_{bj}}$ is the hysteresis force, $f_{ahj,x_{bj}}=-k_a z_j$; z_j is the *effective* hysteresis displacement; V_j is the voltage applied to the jth actuator; k_a and d_a are the mechanical stiffness and effective piezoelectric coefficients that are found as [4, 5, 11, 13]

$$k_a=\frac{1}{4(e_2^U+e_2^M+e_2^L)},\ d_a=-\frac{e_1^U+e_1^M+e_1^L}{h_p},$$

$$e_1^U=\frac{l^2 w}{16I_e}\left(\frac{k_1^U h_p^2}{2E_p}+\frac{k_1^U h_m h_p}{2E_p}-\frac{k_2^U h_p^3}{3E_p}-\frac{k_2^U h_m h_p^2}{4E_p}-\frac{d_{31}h_p^2}{2}-\frac{d_{31}h_m h_p}{2}\right),$$

$$e_2^U=\frac{l^3 w}{192E_p I_e^2}\left(\frac{h_p^3}{3}+\frac{h_m h_p^2}{2}+\frac{h_m^2 h_p}{4}\right),\ e_1^M=-\frac{l^2 w k_2^M h_m^3}{192E_p I_e},\ e_2^M=\frac{E_m l^3 w h_m^3}{2304(E_p I_e)^2},$$

$$e_1^L=\frac{l^2 w}{16I_e}\left(-\frac{k_1^L h_p^2}{2E_p}-\frac{k_1^L h_m h_p}{2E_p}+\frac{k_2^L h_p^3}{6E_p}+\frac{k_2^L h_m h_p^2}{4E_p}-\frac{d_{31}h_p^2}{2}-\frac{d_{31}h_m h_p}{2}\right),$$

$$e_2^L=\frac{l^3 w}{192E_p I_e^2}\left(\frac{h_p^3}{3}+\frac{h_m h_p^2}{2}+\frac{h_m^2 h_p}{4}\right),$$

$$I_e=\frac{w h_p^3}{6}+2h_p w\left(\frac{h_p+h_m}{2}\right)^2+\frac{E_m w h_m^3}{12E_p},$$

$$k_1^U=\frac{(E_p E_m h_m^3+8E_p^2 h_p^3+6E_p^2 h_p^2 h_m)d_{31}}{E_m h_m^3+8E_p h_p^3+12E_p h_p^2 h_m+6E_p h_p h_m^2},$$

$$k_2^U=\frac{12E_p^2 h_p(h_p+h_m)d_{31}}{E_m h_m^3+8E_p h_p^3+12E_p h_p^2 h_m+6E_p h_p h_m^2},$$

$$k_1^M=\frac{6E_m h_m E_p h_p(h_p+h_m)d_{31}}{E_m h_m^3+8E_p h_p^3+12E_p h_p^2 h_m+6E_p h_p h_m^2},$$

$$k_2^M=\frac{12E_m E_p h_p(h_p+h_m)d_{31}}{E_m h_m^3+8E_p h_p^3+12E_p h_p^2 h_m+6E_p h_p h_m^2},$$

$$k_1^L=\frac{(-E_p E_m h_m^3+4E_p^2 h_p^3+6E_p^2 h_p^2 h_m)d_{31}}{E_m h_m^3+8E_p h_p^3+12E_p h_p^2 h_m+6E_p h_p h_m^2},$$

$$k_2^L=\frac{12E_p^2 h_p(h_p+h_m)d_{31}}{E_m h_m^3+8E_p h_p^3+12E_p h_p^2 h_m+6E_p h_p h_m^2};$$

w and l are the width and length of the PZT actuator; h_p is the thickness of piezoelectric layer; h_m is the thickness of the separating layer (e.g., Pt, Fe, polymers, etc.); E_p is the elastic modulus of piezoelectric layer; E_m is the elastic modulus of the separating layer; d_{31} is the piezoelectric strain constant; I_e is effective moment of inertia of the multi-layered composite PZT structure.

The *effective* hysteresis displacement is modeled using the following differential equation

$$\dot{z}_j=k_{ra}d_a\dot{V}_j-k_{sa}z_j\left|\dot{V}_j\right|+k_v\left|z_j\right|\dot{V}_j,$$

where k_{ra} is the restoring force; k_{sa} and k_v are hysteresis shape actuator coefficients.

The following nonlinear differential equations describe the transient dynamics of PZT actuators

$$\dot{x}_{aj}=v_j,$$

$$\dot{v}_j=\frac{1}{m_a}(-k_a x_{aj}-b_a v_j-k_a z_j+k_a d_a V_j),$$

$$\dot{z}_j=k_{ra}d_a\dot{V}_j-k_{sa}z_j\left|\dot{V}_j\right|+k_v\left|z_j\right|\dot{V}_j,$$

where x_{aj} is the actuator displacement.

Hence, the mathematical model of the flexible beam with N surface-mounted PZT actuators is given by

$$\frac{\partial^2 w}{\partial t^2}+2\zeta\sqrt{\frac{EI}{\rho A}}\frac{\partial^3 w}{\partial x^2\partial t}+\frac{EI}{\rho A}\frac{\partial^4 w}{\partial x^4}$$

$$=\frac{1}{\rho A}\sum_{j=1}^{N}\delta(x-x_{bj})\left[k_a d_a V_j-k_a z_j+f_{dj,x_{bj}}\right],$$

where $f_{dj,x_{bj}}$ is the *effective* disturbances force that includes the *equivalent* disturbance at x_{bj}, beam-actuator interaction and noise, $f_{dj,x_{bj}}=f_{disturbances j,x_{bj}}+f_{beam-actuator j,x_{bj}}+\xi_{j,x_{bj}}$.

In the derived mathematical model, f_d is approximated by the disturbance forces $f_{dj,x_{bj}}$, where the noise term $\xi_{j,x_{bj}}$ represents the disturbances from the external forces.

The state-space model is given by the following set of differential equations

$$\dot{x}_{i1}=x_{i2},$$

$$\dot{x}_{i2}=-\omega_i^2 x_{i1}-2\zeta\omega_i x_{i2}+\sum_{j=1}^{N}\Phi_i(x_{bj})\left[k_a d_a V_j-k_a z_j+f_{dj,x_{bj}}\right],$$

$$\dot{z}_j=k_{ra}d_a\dot{V}_j-k_{sa}z_j\left|\dot{V}_j\right|+k_v\left|z_j\right|\dot{V}_j.$$

VI. Tracking Control Laws Design

A high-fidelity mathematical model of the pointing systems was derived in the form of nonlinear differential equations. Furthermore, the actuators (brushless permanent-magnet

servomotors and PZT actuators) were examined. This section is devoted to outline the basic fundamentals in the design of robust control laws in order to guarantee the optimal performance of flexible pointing systems. Using the conventional state-space notations [10, 12], the linear and nonlinear systems dynamics are modeled as

$$\dot{x}^{sys}(t) = A^{sys}x^{sys} + B^{sys}u,\ y = Hx^{sys},$$
$$\dot{x}^{sys}(t) = F(x^{sys}) + B(x^{sys})u,\ y = H(x^{sys}). \quad (1)$$

The tracking error vector is given as

$$e(t) = Nr(t) - y(t) = Nr(t) - Hx^{sys}(t). \quad (2)$$

From (2), taking note of (1), one obtains

$$\dot{e}(t) = N\dot{r}(t) - \dot{y}(t) = N\dot{r}(t) - H\dot{x}^{sys}(t) = N\dot{r}(t) - HA^{sys}x^{sys} - HB^{sys}u. \quad (3)$$

Using the expanded state vector $x(t) = \begin{bmatrix} x^{sys}(t) \\ e(t) \end{bmatrix}$, we have

$$\dot{x}(t) = \begin{bmatrix} \dot{x}^{sys}(t) \\ \dot{e}(t) \end{bmatrix} = \begin{bmatrix} A^{sys} & 0 \\ -HA^{sys} & 0 \end{bmatrix}\begin{bmatrix} x^{sys} \\ e \end{bmatrix} + \begin{bmatrix} B^{sys} \\ -HB^{sys} \end{bmatrix}u + \begin{bmatrix} 0 \\ N \end{bmatrix}\dot{r} = \quad (4)$$

$$Ax + Bu + \begin{bmatrix} 0 \\ N \end{bmatrix}\dot{r},\ y = Hx^{sys}$$

We introduce the *state transformation* method to design robust controllers [10]. The following z and v variables

$$z = \begin{bmatrix} x \\ u \end{bmatrix} \text{ and } v = \dot{u} \quad (5)$$

are used.

From (5), for linear systems (1), one has

$$\dot{z}(t) = \begin{bmatrix} A & B \\ 0 & 0 \end{bmatrix}z + \begin{bmatrix} 0 \\ I \end{bmatrix}v = A_z z + B_z v,\ y = Hx^{sys},\ z(t_0) = z_0. \quad (6)$$

Minimizing the quadratic functional

$$J = \int_{t_0}^{t_f}\left(z^T Q_z z + v^T G_z v\right)dt,\ Q_z \geq 0,\ G>0, \quad (7)$$

and using the quadratic return function $V(z) = z^T Kz$, the application of the first-order necessary condition for optimality gives

$$v = -G_z^{-1}B_z^T Kz. \quad (8)$$

The unknown matrix K is found by solving the Ricatti equation [10, 12]

$$-\dot{K} = KA_z + A_z^T K - KB_z G_z^{-1}B_z^T K + Q_z,\ K(t_f) = K_f. \quad (9)$$

Using (5) and (8), one has

$$\dot{u}(t) = -G_z^{-1}B_z^T Kz = -G_z^{-1}\begin{bmatrix} 0 \\ I \end{bmatrix}^T\begin{bmatrix} K_{11} & K_{21}^T \\ K_{21} & K_{22} \end{bmatrix}\begin{bmatrix} x \\ u \end{bmatrix} = \quad (10)$$

$$-G_z^{-1}K_{21}x - G_z^{-1}K_{22}u = K_{f1}x + K_{f2}u.$$

From $\dot{x}(t) = Ax + Bu$, we have $u = B^{-1}\left(\dot{x}(t) - Ax\right)$.

Thus, one obtains

$$u = B^{-1}\left(\dot{x}(t) - Ax\right) = \left(B^T B\right)^{-1}B^T\left(\dot{x}(t) - Ax\right). \quad (11)$$

From (10) and (11), we have

$$\dot{u}(t) = K_{f1}x + K_{f2}u = K_{f1}x + K_{f2}\left(B^T B\right)^{-1}B^T\left(\dot{x}(t) - Ax\right)$$
$$= \left[K_{f1} - K_{f2}\left(B^T B\right)^{-1}B^T A\right]x(t) + K_{f2}\left(B^T B\right)^{-1}B^T\dot{x}(t) \quad (12)$$
$$= \left(K_{f1} - K_{F1}A\right)x(t) + K_{F1}\dot{x}(t) = K_{F2}x(t) + K_{F1}\dot{x}(t).$$

From (12), one obtains the controller as

$$u(t) = K_{F1}x(t) - K_{F1}x_0 + \int K_{F2}x(\tau)d\tau + u_0. \quad (13)$$

It is obvious that the designed control law (13) is the proportional-integral controller with state feedback because

$$x(t) = \begin{bmatrix} x^{sys}(t) \\ e(t) \end{bmatrix}.$$

For nonlinear pointing systems, that are described by differential equations in state-space form (2), the proposed procedure is straightforwardly used. In particular, one has the following equation that defines the control law

$$\dot{u}(t) = -G_z^{-1}B_z^T\frac{\partial V}{\partial z} = -G_z^{-1}\begin{bmatrix} 0 \\ I \end{bmatrix}^T\frac{\partial V(x,u)}{\partial[x\ \ u]^T}, \quad (14)$$

where $V(x,u)$ is the return function.

Distinct nonquadratic functionals, for example

$$J = \int_{t_0}^{t_f}\left(\sum_{i=0}^{\zeta}\frac{2\eta+1}{2(\kappa i+\eta+1)}z^{\frac{\kappa i+\eta+1}{2\eta+1}^T}Q_{zi}z^{\frac{\kappa i+\eta+1}{2\eta+1}} + v^T G_z v\right)dt,$$

can be used to attain the desired performance [12]. If the solution of the Hamilton-Jacobi equation can be approximated by the quadratic return function, the controller (13) results.

VII. Tracking Controler Design For PZT Actuators

We study the flexible pointing system with surface-mounted PZT actuators. The parameters of piezoelectric bimorph G-1195, Piezo Systems Inc. PZT actuators are: w = 10 mm, l = 10 mm, h_p = 0.35 mm, h_m = 0.25 mm, $E_p = 6.1\times10^{10}$ N/m^2, $E_m = 1.93\times10^{11}$ N/m^2 and $d_{31} = 320\times10^{-12}$ m/V.

Making use of the reported *state transformation* method, the tracking controller is synthesized as

$$\dot{u} = -K_f\mathbf{x},\ u = V = -K_f\frac{1}{s}\mathbf{x},$$

where K_f is the matrix of feedback coefficients, $K_f \in \mathbb{R}^{1\times4}$.

The augmented vector $\mathbf{x}(t) = \left[x(t)\ \ v(t)\ \ e(t)\ \ V(t)\right]^T$ is used. Assigning the weighting matrices to be

$$Q = \begin{bmatrix} 1 & 0 & 0 & 0 \\ 0 & 1 & 0 & 0 \\ 0 & 0 & 3\times10^{24} & 0 \\ 0 & 0 & 0 & 1 \end{bmatrix} \text{ and } G = 10,$$

the feedback matrix K_f is found as [4, 5]

$$K_f = \left[-9.9\times10^{11}\ \ 2.6\times10^{6}\ \ -5.5\times10^{11}\ \ 1.6\times10^{4}\right].$$

The actuator dynamics for $-150 \leq V_j \leq 150$ V when the reference displacements are ± 0.0001 mm are illustrated in Figure 3. The integration of saturation and hysteresis phenomena ensure correctness of results.

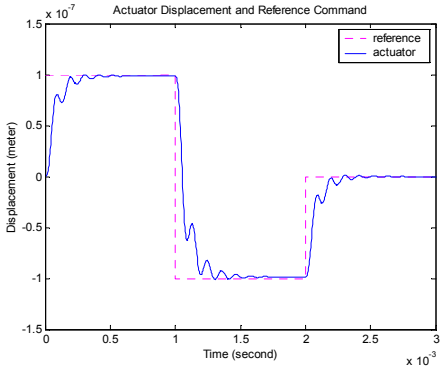

Figure 3. Dynamics of the PZT actuator for different commands

VIII. Tracking Controlers For Pointing Systems

In this paper we examine the flexible pointing system with three surface-mounted PZT actuators. The differential equations that model the flexible beam are

$$\dot{x}_{i1} = x_{i2},$$

$$\dot{x}_{i2} = -\omega_i^2 x_{i1} - 2\zeta\omega_i x_{i2} + k_a d_a \sum_{j=1}^{3} \Phi_i(x_{bj}) V_j .$$

The following state-space form model results

$$\begin{bmatrix} \dot{x}_1 \\ \vdots \\ \dot{x}_n \end{bmatrix} = \begin{bmatrix} \omega_1 & 0 & 0 \\ 0 & \ddots & 0 \\ 0 & 0 & \omega_n \end{bmatrix} \begin{bmatrix} x_1 \\ \vdots \\ x_n \end{bmatrix} + \begin{bmatrix} 0 & 0 & 0 \\ \Phi_1(x_{b1}) & \Phi_1(x_{b2}) & \Phi_1(x_{b3}) \\ \vdots & \vdots & \vdots \\ 0 & 0 & 0 \\ \Phi_n(x_{b1}) & \Phi_n(x_{b2}) & \Phi_n(x_{b3}) \end{bmatrix} \begin{bmatrix} f_{a1,x_{b1}} \\ f_{a2,x_{b2}} \\ f_{a3,x_{b3}} \end{bmatrix}$$

where the forces developed by the surface-mounted PZT actuator are found as

$$\begin{bmatrix} f_{a1,x_{b1}} \\ f_{a2,x_{b2}} \\ f_{a3,x_{b3}} \end{bmatrix} = k_a d_a \begin{bmatrix} V_1 \\ V_2 \\ V_3 \end{bmatrix}.$$

The parameters of the flexible beam with PZT actuators are reported in Table 1.

TABLE 1
PARAMETERS OF THE FLEXIBLE BEAM WITH PZT ACTUATORS

Notation	Numerical Value
Beam length (l)	1 m
Young's modulus (E)	2.7×10^{10} N/m^2
Moment of inertia about z-axis (I)	1.6×10^{-9} m^4
Density of beam material (ρ)	1.7×10^{3} kg/m^3
Cross-sectional area (A)	0.6×10^{-3} m^2
Damping coefficient (ζ)	0.1
Actuator mass (m_a)	0.7×10^{-3} kg
Actuator damping constant (b_a)	1 N-sec/m
Actuator mechanical stiffness (k_a)	2.2×10^{6} N/m
Piezoelectric coefficient (d_a)	1.6×10^{-8} m/V
Restoring force coefficient (k_{ra})	0.0075
Hysteresis shape coefficient (k_{sa})	0.03
Hysteresis shape coefficient (k_v)	0.003
White noise power ξ (distributed disturbance force)	5×10^{-4}

Nonlinear simulations and data-intensive analysis are performed using the mathematical model reported. Let the number of modes is six, e.g., n=6. In simulation and analysis, we examine the beam deflections w_1, w_2 and w_3 (measured at the positions of the applied forces $f_{a1,x_{b1}}$, $f_{a2,x_{b2}}$ and $f_{a3,x_{b3}}$).

The dynamics of the open-loop pointing system are plotted in Figure 4.

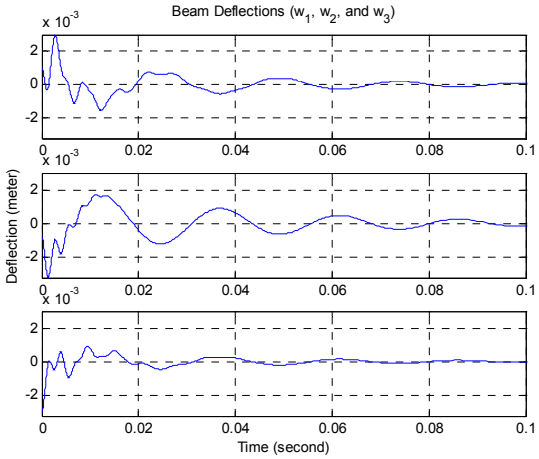

Figure 4. Pointing system deflections at 0.40, 0.75 and 0.95 m

The procedure to design tracking controllers was reported in section VI using the *state transformation* method. It must be emphasized that stabilizing controllers can be straightforwardly synthesized [10, 12]. In this section we first design stabilizing controllers, and then derive tracking controllers. The quadratic functionals and return functions are used to find the control laws.

The stabilizing controllers are designed to attenuate the flexible modes, and these controllers cannot ensure the tracking needed. The stabilizing controller is given as

$$u = -K_p x_p,$$

$$x_p = [x_{11} \quad x_{12} \quad x_{21} \quad x_{22} \quad x_{31} \quad x_{32} \quad x_{41} \quad x_{42} \quad x_{51} \quad x_{52} \quad x_{61} \quad x_{62}]^T$$

where K_p is the matrix of feedback coefficients.

Assigning the weighting coefficients to be q_{ii}=5000 and g_{ii}=1, we have the feedback coefficient matrix

$$K_p = \begin{bmatrix} 9.96 & -24.94 & -9.13 \\ 51.13 & 36.80 & 7.99 \\ -607.62 & -21.49 & 81.72 \\ 23.31 & -38.08 & -11.62 \\ -1.03\times10^{3} & 1.77\times10^{3} & 589.43 \\ -14.91 & 17.56 & 11.69 \\ -1.43\times10^{3} & -364.56 & 44.49 \\ -15.11 & -3.32\times10^{-2} & -9.47 \\ 145.87 & -444.11 & -165.39 \\ 3.75\times10^{-4} & -7.53 & 7.56 \\ 855.47 & 745.70 & 18.98 \\ 7.04 & 7.39 & -5.99 \end{bmatrix}^T .$$

For the studied beam, we place PZT actuators at 0.40, 0.75 and 0.95 meters from the fixed (clamped) end. This actuator location guarantees the optimality from the viewpoint of overall system performance. Figure 5 illustrates the beam dynamics at the actuators positions (0.40, 0.75 and 0.95 meters) assuming that ideal point forces are applied to stabilize the beam. The applied forces developed by the PZT actuators are bounded. These constraints $-5 \le f_{aj} \le 5$ N are integrated in the analysis to guarantee correctness of modeling and simulation results. It is evident that the stabilizing controller ensure stabilization as well as vibration and disturbance attenuation. The settling time is 0.06 sec, while for open-loop system the settling time was 0.1 sec, see Figures 4 and 5.

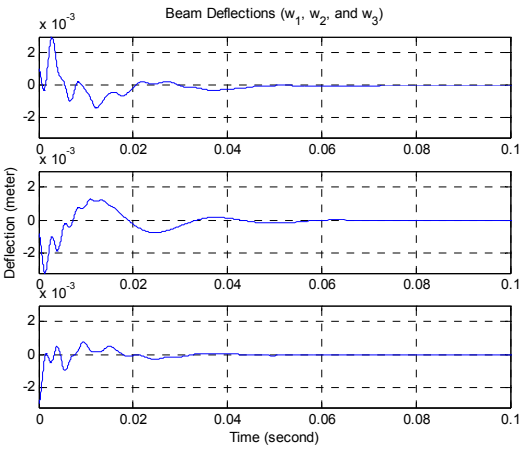

Figure 5. Deflections of the closed-loop pointing system with stabilizing control

To attain high-fidelity modeling, data-intensive analysis and accuracy of results, the closed-loop pointing systems must be analyzed by integrating PZT actuators with stabilizing and tracking control laws.

Figure 6 illustrates the simulation results for the pointing system utilizing high-fidelity PZT actuators model. The resulting forces for surface-mounted PZT actuators are

$$f_{j,x_{bj}}(t) = f_{aj,x_{bj}} + f_{ahj,x_{bj}} = k_a d_a V_j - k_a z_j .$$

To attain the desired performance for the flexible beam, the weighting coefficients were assigned as $q_{ii}=5\times10^7$and $g_{ii}=1$. The feedback coefficients matrix is found to be

$$K_p = \begin{bmatrix} -2.74\times10^3 & -2.96\times10^3 & -1.38\times10^3 \\ 5.67\times10^3 & 3.77\times10^3 & 658.31 \\ -1.77\times10^5 & 1.08\times10^5 & 6.37\times10^4 \\ 3.14\times10^3 & -4.93\times10^3 & -1.32\times10^3 \\ -6.16\times10^5 & 8.96\times10^5 & 3.08\times10^5 \\ -2.46\times10^3 & 2.58\times10^3 & 2.30\times10^3 \\ -1.10\times10^6 & -2.70\times10^5 & 9.72\times10^4 \\ -3.27\times10^3 & -55.83 & -2.30\times10^3 \\ 3.94\times10^5 & -3.36\times10^5 & -1.87\times10^5 \\ -47.76 & -2.04\times10^3 & 2.11\times10^3 \\ 9.89\times10^5 & 8.72\times10^5 & -1.78\times10^5 \\ 1.92\times10^3 & 1.96\times10^3 & -1.63\times10^3 \end{bmatrix}^{\mathrm{T}} .$$

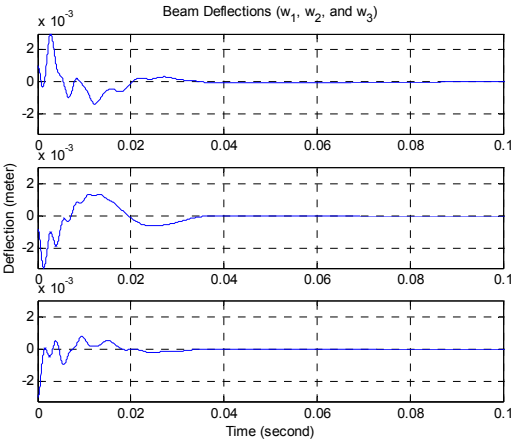

Figure 6. Deflections of the closed-loop pointing system

The nonlinear phenomena (saturation, hysteresis, etc.) degrade the pointing system dynamic, steady-state performance, dynamic and steady-sate accuracy, settling time, etc. The results reported for the closed-loop system with the synthesized stabilizing controller, as shown in Figure 6, provide the evidence that the designed controller guarantees good performance and stability. It is apparent that vibration and disturbance attenuations are achieved. The settling time is 0.04 sec (for open-loop system, the settling time was 0.1 sec, see Figure 4).

We focus our attention on the design of tracking control laws. Our goal not only to guarantee vibration and disturbance attenuation, but also ensure accurate tracking precisely positioning the pointing system. To attain precise angular positioning, the tracking control problem is solved for the flexible pointing system applying the *state transformation* method. The tracking control is found as

$$\dot{u} = -K_t \mathbf{x}, \qquad u = V = -K_t \frac{1}{s}\mathbf{x}, \qquad \mathbf{x}(t) = \begin{bmatrix} x_i(t) \\ e_j(t) \\ V_j(t) \end{bmatrix}$$

We denote $x_i=[x_{i1}\ \ x_{i2}]^{\mathrm{T}}$; i=1, … ,6 (n=6), and j = 1, 2, 3 (N = 3).

The extended state vector that integrates state variables is $x(t)$ =

$$[x_{11}\ x_{12}\ x_{21}\ x_{22}\ x_{31}\ x_{32}\ x_{41}\ x_{42}\ x_{51}\ x_{52}\ x_{61}\ x_{62}\ e_1\ e_2\ e_3\ V_1\ V_2\ V_3]^T$$

The matrix of feedback coefficients $K_f \in \mathbb{R}^{3\times18}$ is found solving the functional differential equation, called Hamilton-Jacobi equation [10, 12]. We use the following weighting coefficients:

q_{ii}=1 (expect $q_{13,13}=q_{14,14}=q_{15,15}=1.25\times10^{17}$) and g_{ii}=10.

Figure 7 documents the dynamics and tracking at the actuator positions assigning the reference displacements at 0.40, 0.75 and 0.95 m to be

$$r = \begin{bmatrix} r_{1\ \text{at 0.40 m}} \\ r_{2\ \text{at 0.75 m}} \\ r_{3\ \text{at 0.95 m}} \end{bmatrix} = \begin{bmatrix} 0.0005\ \text{m} \\ -0.0005\ \text{m} \\ 0.0015\ \text{m} \end{bmatrix}.$$

Therefore, the tracking performance is examined assigning the desired command deflections.

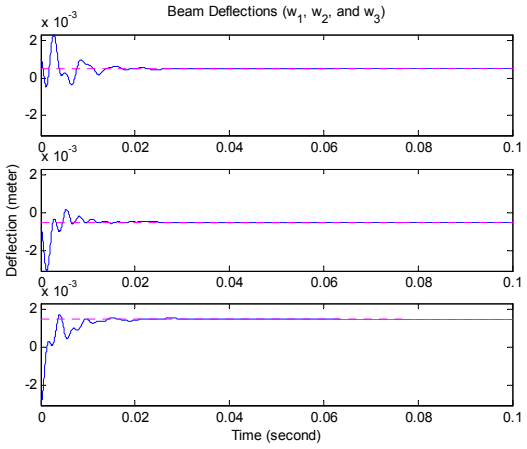

Figure 7. Tracking of the closed-loop pointing system with tracking controller

The actuator dynamics must be integrated in the modeling and simulations to study the closed-loop pointing system performance attaining data-intensive analysis.

The synthesis of the tracking control law is performed by assigning the weighting coefficients to be:

q_{ii}=1 (expect $q_{13,13}$=$q_{14,14}$=$q_{15,15}$=6×10^{21}) and g_{ii}=100.

The closed-loop dynamics of the flexible pointing system for the specified command displacements (0.0005, –0.0005 and 0.0015 meters) are illustrated in Figure 8.

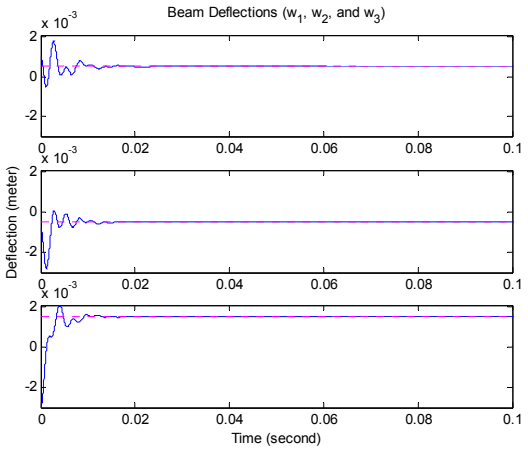

Figure 8. Tracking of the flexible pointing system

The analysis documented provides the evidence that high-accuracy fast tracking, stabilization and disturbance attenuation are achieved. The settling time is 0.02 second. We conclude that the optimal *achievable* performance was accomplished within the "performance deteriorating" nonlinear phenomena, e.g., hysteresis, bounds, constraints, etc.

IX. Nonlinear Optimization

In this section we examine and solve the optimal actuator placement problem. To examine the performance of the closed-loop pointing system with three actuators, the performance functional must be examined. In particular, this functional should *map* the overall pointing system performance. The pointing system accuracy, deflection, settling time, overshoot, force, and other performance characteristics can be straightforwardly integrated. For example, using the beam deflections and settling time, the performance functional is assigned as

$$J_{PF} = q_{tt}\left(t_{1settling} + t_{2settling} + t_{3settling}\right) + \int_{t_0}^{t_{settling\,\max}} q_{tw} t\left(\left| w_1(t,x)\right| + \left| w_2(t,x)\right| + \left| w_3(t,x)\right|\right)dt,$$

where q_{tt} and q_{tw} are the weighting coefficients.

Nonlinear simulations for the closed-loop pointing system give the values of the J_{PF}. The performance functional was examined for different locations of the first and second PZT actuators denoted as x_{b1} and x_{b2}. The third PZT actuator was positioned at 0.95 m, e.g., x_{b3}=0.95 m. The weighting coefficients influence the $J_{PF}(x_{b1},x_{b2})$, and q_{tt}, q_{tw} must be chosen based upon the performance requirements and specifications. We assign q_{tt}=1 and q_{tw}=5×10^5 to attain the weighted performance specifications equivalency. The heterogeneous simulations and data-intensive analysis are performed in the MATLAB environment [5]. The three-dimensional plot for $J_{PF}(x_{b1},x_{b2})$ found and illustrated in Figure 9.

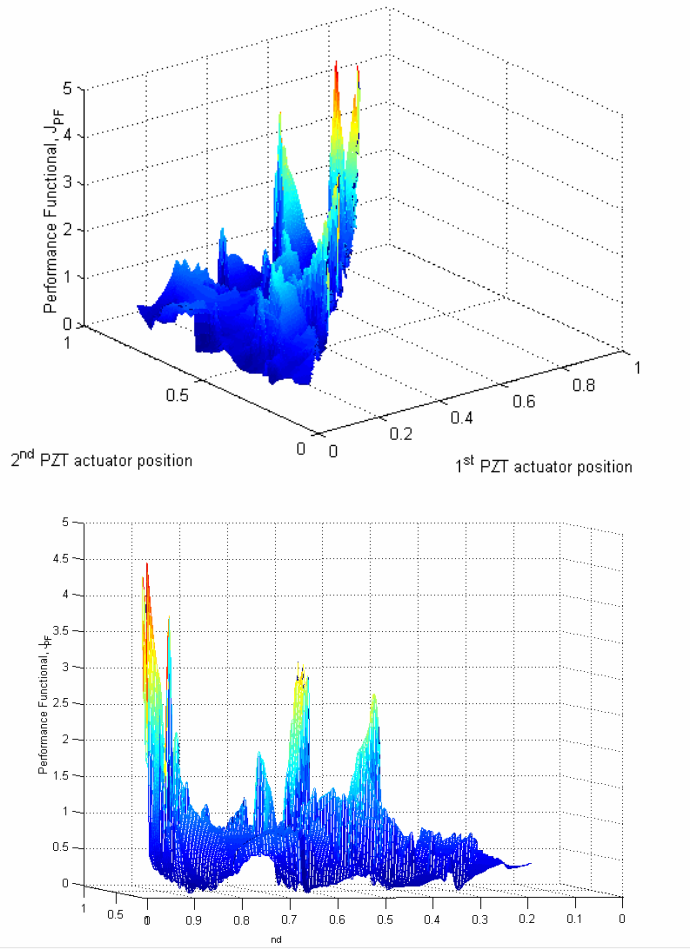

Figure 9. Performance functional $J_{PF}(x_{b1},x_{b2})$ if x_{b3}=0.95 m

The optimum locations, which correspond to the minimum values of performance functional $J_{PF}(x_{b1},x_{b2})$, are found. The value for $J_{PF}(x_{b1},x_{b2})$ is a function of locations of first and second PZT actuators x_{b1} and x_{b2}. Figure 9 illustrates the variations of $J_{PF}(x_{b1},x_{b2})$ in three dimensions. Six optimal locations with the corresponding values of $J_{PF}(x_{b1},x_{b2})$, which was minimized, are documented in Table 2. The locations of first and second PZT actuators x_{b1} and x_{b2} that guarantee minimum for $J_{PF}(x_{b1},x_{b2})$ are documented.

TABLE 2
OPTIMAL LOCATIONS FOR THE FIRST AND SECOND PZT ACTUATORS

$J_{PF}(x_{b1},x_{b2})$	Location of x_{b1}	Location of x_{b2}
0.082	0.34	0.86
0.085	0.48	0.66
0.095	0.16	0.86
0.1	0.34	0.46
0.103	0.66	0.86
0.104	0.46	0.85

Let us examine the numerical results reported in Figure 9 and Table 2. It is evident that the maximum value for $J_{PF}(x_{b1},x_{b2})$ was found to be 4.5 if the PZT actuators are placed at x_{b1}=0.75, x_{b2}=0.9 and x_{b3}=0.95 m. Correspondingly, these actuator locations correspond to the worst-case actuators placement. The minimum value of $J_{PF}(x_{b1},x_{b2})$ is found if x_{b1}=0.34, x_{b2}=0.86 and x_{b3}=0.95 m.

Design and analysis of the flexible pointing system were performed for x_{b1}=0.40, x_{b2}=0.75 and x_{b3}=0.95 m. This actuators location corresponds to other weighting coefficients q_{tt} and q_{tw} of the performance functional. The results reported provide the evidence that $J_{PF}(x_{b1},x_{b2})$ is a nonlinear function of x_{b1} and x_{b2}. Furthermore, the robustness and sensitivity must be also integrated in the design in order to optimize the actuator locations.

The animations were performed in the MATLAB environment [5]. The results are documented in Figure 10 at the time instants 0.001, 0.01, 0.03 and 0.07 seconds.

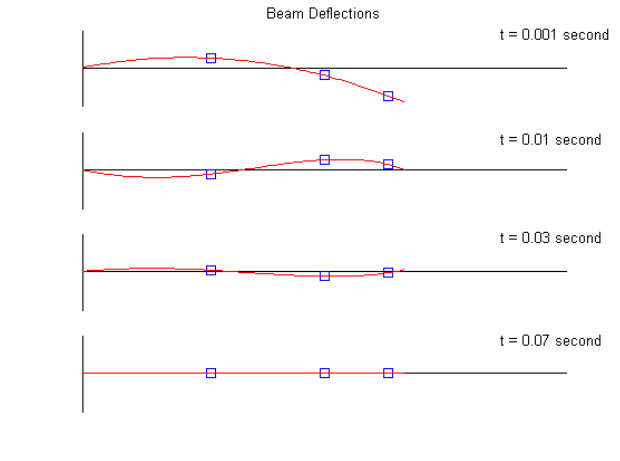

Figure 10. Deflection of flexible pointing system with three surface-mounted PZT actuators

High-fidelity modeling, nonlinear simulations, and data-intensive analysis fully support the design paradigms reported. The results provide the designer with the novel concepts in analysis, design and optimization of high-performance pointing systems. The direct implementation of fundamental and applied research and developments can be transferred to flexible robots, aerospace structures, marine kinematics, etc. The developed software fully supports data-intensive analysis, heterogeneous simulation, robust design, virtual prototyping and interactive visualization of the results. The developed software can be used in the development of computer-aided-design software that will support heterogeneous simulation, data-intensive analysis with outcome prediction, coherent design, nonlinear optimization and interactive visualization.

X. CONCLUSIONS

In this paper accurate positioning, vibration reduction and disturbance attenuations problems were addressed and solved for flexible pointing systems with surface-mounted PZT actuators. To coherently examine these problems, high-fidelity mathematical modeling, heterogeneous simulation, data-intensive analysis, robust control and optimization issues were thoroughly studied. The high-performance pointing system hardware was synthesized utilizing advanced actuators, sensors and electronics. The mathematical models are described by partial differential equations, and nonlinear actuator dynamics are integrated to perform design, analysis and optimization. Forces, developed by the surface-mounted PZT actuators, are applied to accurately position and stabilize the pointing system, as well as attenuate vibrations, and minimize disturbances. High-fidelity mathematical models of actuators are examined because nonlinearities, hysteresis and other phenomena cannot be neglected. To guarantee the optimal performance, robust stabilizing and tracking controllers are designed. The multi-objective nonlinear parametric optimization problem was solved examining the system performance by using different number of actuators and optimizing their locations. The proposed mathematical models, design and optimization paradigms are verified through heterogeneous simulations and data-intensive analysis using the MATLAB environment. The developed software can be used in the development of computer-aided-design software for flexible pointing systems. Novel fundamental, applied and experimental results reported enhance the horizon in modeling, analysis and design flexible pointing systems.

REFERENCES

[1] D. Allaei, D. J. Tarnowski, M. S. Mattice and R. Testa "Smart isolation mount for army guns – Part 1: preliminary results," *Proc. SPIE Conf. Smart Structures and Materials 2000: Smart Electronics and MEMS,* pp. 70-77, 2000.

[2] F. Khorrami, S. Jain, M. Mattice and N. Coleman, "Rapid retargeting of a flexible pointing system with structure mounted sensors and actuators," *Proc. American Control Conf.,* San Francisco, CA, vol. 3, pp. 1632-1636, 1993.

[3] A. Hac and L. Liu, "Sensor and actuator location in motion control of flexible structures," *Journal of Sound and Vibration*, vol. 167, no. 2, pp. 239-261, 1993.

[4] S. E. Lyshevski and J. Getpreecharsawas, "Surface-mounted thin-film actuators in pointing systems," *Proc. IEEE Conference on Nanotechnology*, pp. 465-470, Washington, DC, 2002.

[5] J. Getpreecharsawas and S. E. Lyshevski, "Modeling and analysis of flexible beams with surface-mounted PZT actuators," *Conference on Decision and Control*, pp. 4593-4598, Las Vegas, NV, 2002.

[6] L. Meirovitch, *Computational Methods in Structural Dynamics.* Sijthoff and Noordhoff, Rockvill, MD, 1980.

[7] W. K. Belvin and K. C. Park, "Structural tailoring and feedback control synthesis: An interdisciplinary approach," *J. Guidance, Control, and Dynamics*, vol. 13, no. 3, p 424-429, 1990.

[8] R. L. Lashlee, V. Rao and F. Kern, "Mixed H_2 and H-optimal control of smart structures," *Proc. Conf. Decision and Control*, Lake Buena Vista, FL, pp. 115-120, 1994.

[9] X. Wang, C. Ehlers and M. Neitzel, "Dynamic analysis of piezoelectric actuator bonded on beam." *Proc. ICIM/ECSSM Conf.*, Lyon, France, pp. 883-890, 1996.

[10] S. E. Lyshevski, *MEMS and NEMS: Systems, Devices, and Structures*, CRC Press, Boca Raton, FL, 2002.

[11] J. G. Smith and Wai-Shing Choi, "The constituent equations of piezoelectric heterogeneous bimorphs," *IEEE Trans. Ultrasonics, Ferroelectrics, and Frequency Control,* vol. 38, no. 3, pp. 256-270, 1991.

[12] S. E. Lyshevski, *Control Systems Theory With Engineering Applications*, Birkh@user, Boston, MA, 2001.

[13] T. S. Low and W. Guo, "Modeling of a three-layer piezoelectric bimoph beam with hysteresis," *Journal of Microelectromechanical Systems*, vol. 4, no. 4, pp. 230-237, 1995.